Introduction

Seismic Interferometry (SI) is the process of generating new seismic responses by cross-correlating existing responses; see Wapenaar et al. (2008) and Schuster (2009) for an overview of this branch of science. One application of SI is to redatum surface sources to downhole receiver locations, a methodology that is widely known as the Virtual Source method (Bakulin and Calvert, 2006). Mehta et al. (2007) showed how separation of up- and downgoing wave fields can improve the redatuming process considerably. We give a formal derivation to support their conclusions and extend them to general inhomogeneous elastodynamic media, yielding a set of representations to redatum decomposed wavefields from their original source locations at the earth surface to downhole receiver locations. The theory is supported with a 2D synthetic example.

Theory

In Figure 1a we give a schematic overview of the configuration. At the surface ∂D_0 we have multi-component sources and at locations $\mathbf{x}_A$ and $\mathbf{x}_B$ in the subsurface we have multi-component receivers. Boundaries ∂D_0 and ∂D_m enclose the volume D. We assume the medium outside D to be homogeneous. In practice this means that free surface related effects and other forms of scattering from above ∂D_0 must be eliminated prior to our analysis. We decompose the data at both source and receiver side and deconvolve with the source wavelet to obtain the decomposed Green's functions that are cast in the following Green's matrices:

$$\hat{\mathbf{\Gamma}}\left(\mathbf{x}_R,\mathbf{x}_S\right)=\begin{pmatrix}\hat{\mathbf{G}}^{+,+}\left(\mathbf{x}_R,\mathbf{x}_S\right) & \hat{\mathbf{G}}^{+,-}\left(\mathbf{x}_R,\mathbf{x}_S\right)\\ \hat{\mathbf{G}}^{-,+}\left(\mathbf{x}_R,\mathbf{x}_S\right) & \hat{\mathbf{G}}^{-,-}\left(\mathbf{x}_R,\mathbf{x}_S\right)\end{pmatrix}, \tag{1}$$

for a source at $\mathbf{x}_S$ and a receiver at $\mathbf{x}_R$. $\hat{\mathbf{G}}^{\pm,\pm}$ is a matrix with the different wave modes (P, Sv or Sh) and their conversions as components. Each column of $\hat{\mathbf{G}}^{\pm,\pm}$ hosts a particular mode excited at the source side, whereas each row of $\hat{\mathbf{G}}^{\pm,\pm}$ hosts a particular mode registered at the receiver side. The first superscript denotes the propagation direction at the receiver location, the second superscript denotes the propagation direction at the source location, where + means downgoing and – means upgoing. All Green's matrices must obey the one-way wave equation: $\partial_3\hat{\mathbf{\Gamma}}\left(\mathbf{x}_R,\mathbf{x}_S\right)=\hat{\mathbf{B}}\hat{\mathbf{\Gamma}}\left(\mathbf{x}_R,\mathbf{x}_S\right)+\mathbf{I}\delta\left(\mathbf{x}_R-\mathbf{x}_S\right)$, where $\hat{\mathbf{B}}$ is a one-way operator matrix, containing the medium parameters and lateral differential operators, $\mathbf{I}$ is an identity matrix and $\delta\left(\mathbf{x}_R-\mathbf{x}_S\right)$ is a delta-function. We consider the interaction quantity $\partial_3\left\{\hat{\mathbf{\Gamma}}^{\dagger}\left(\mathbf{x},\mathbf{x}_A\right)\mathbf{J}\hat{\mathbf{\Gamma}}\left(\mathbf{x},\mathbf{x}_B\right)\right\}$, where $\mathbf{J}=\begin{pmatrix}\mathbf{I} & \mathbf{0}\\ \mathbf{0} & -\mathbf{I}\end{pmatrix}$, $\mathbf{0}$ is a zero matrix, superscript $\dagger$ is the complex conjugate transpose and ∂_3 is a spatial derivative to depth. Next we take the product rule of the interaction quantity, substitute the one way wave equation into the result and apply the theorem of Gauss. This yields boundary integrals over ∂D_0 and ∂D_m and a volume integral. We assume that ∂D_m is deep enough below a 'sufficiently inhomogeneous medium', so that its contribution can be neglected (Wapenaar, 2006). We use the symmetry property $\hat{\mathbf{B}}^{\dagger}\mathbf{J}\approx-\mathbf{J}\hat{\mathbf{B}}$, where the evanescent wavefield is neglected. We transpose the result, followed by applying symmetry properties $\mathbf{J}^T=\mathbf{J}^{-1}=\mathbf{J}$, $\left\{\hat{\mathbf{\Gamma}}\left(\mathbf{x}_R,\mathbf{x}_S\right)\right\}^T=\mathbf{N}\hat{\mathbf{\Gamma}}\left(\mathbf{x}_S,\mathbf{x}_R\right)\mathbf{N}$ (with $\mathbf{N}=\begin{pmatrix}\mathbf{0} & \mathbf{I}\\ -\mathbf{I} & \mathbf{0}\end{pmatrix}$), $\mathbf{JN}=-\mathbf{NJ}$ and $\mathbf{N}^{-1}=\mathbf{N}^T=-\mathbf{N}$, to arrive at

$$\hat{\mathbf{\Gamma}}\left(\mathbf{x}_B,\mathbf{x}_A\right)+\mathbf{J}\hat{\mathbf{\Gamma}}^{\dagger}\left(\mathbf{x}_A,\mathbf{x}_B\right)\mathbf{J}=\int_{\partial D_0}\hat{\mathbf{\Gamma}}\left(\mathbf{x}_B,\mathbf{x}\right)\mathbf{J}\hat{\mathbf{\Gamma}}^{\dagger}\left(\mathbf{x}_A,\mathbf{x}\right)\mathbf{J}d^2\mathbf{x}\,. \tag{2}$$

As we assume all free surface related effects to have been removed (thus the medium above ∂D_0 is homogeneous), all relevant wavefields excited from $\mathbf{x}$ are purely downgoing; thus $\hat{\mathbf{G}}^{\pm,-}\left(\mathbf{x}_{A/B},\mathbf{x}\right)=0$. Substituting this with equation 1 into equation 2 yields:

$$\hat{\mathbf{G}}^{-,+}\left(\mathbf{x}_B,\mathbf{x}_A\right)-\left\{\hat{\mathbf{G}}^{+,-}\left(\mathbf{x}_A,\mathbf{x}_B\right)\right\}^{\dagger}=\int_{\partial D_0}\hat{\mathbf{G}}^{-,+}\left(\mathbf{x}_B,\mathbf{x}\right)\left\{\hat{\mathbf{G}}^{+,+}\left(\mathbf{x}_A,\mathbf{x}\right)\right\}^{\dagger}d^2\mathbf{x}\,, \tag{3}$$

$$\hat{\mathbf{G}}^{+,-}\left(\mathbf{x}_B,\mathbf{x}_A\right)-\left\{\hat{\mathbf{G}}^{-,+}\left(\mathbf{x}_A,\mathbf{x}_B\right)\right\}^{\dagger}=-\int_{\partial D_0}\hat{\mathbf{G}}^{+,+}\left(\mathbf{x}_B,\mathbf{x}\right)\left\{\hat{\mathbf{G}}^{-,+}\left(\mathbf{x}_A,\mathbf{x}\right)\right\}^{\dagger}d^2\mathbf{x}\,, \tag{4}$$

$$\hat{\mathbf{G}}^{+,+}\left(\mathbf{x}_B,\mathbf{x}_A\right)+\left\{\hat{\mathbf{G}}^{+,+}\left(\mathbf{x}_A,\mathbf{x}_B\right)\right\}^{\dagger}=\int_{\partial D_0}\hat{\mathbf{G}}^{+,+}\left(\mathbf{x}_B,\mathbf{x}\right)\left\{\hat{\mathbf{G}}^{+,+}\left(\mathbf{x}_A,\mathbf{x}\right)\right\}^{\dagger}d^2\mathbf{x}\,, \tag{5}$$

$$\hat{\mathbf{G}}^{-,-}\left(\mathbf{x}_B,\mathbf{x}_A\right)+\left\{\hat{\mathbf{G}}^{-,-}\left(\mathbf{x}_A,\mathbf{x}_B\right)\right\}^{\dagger}=-\int_{\partial D_0}\hat{\mathbf{G}}^{-,+}\left(\mathbf{x}_B,\mathbf{x}\right)\left\{\hat{\mathbf{G}}^{-,+}\left(\mathbf{x}_A,\mathbf{x}\right)\right\}^{\dagger}d^2\mathbf{x}\,. \tag{6}$$

The use of equation 3 is demonstrated in Figure 2a. The downgoing field at $\mathbf{x}_A$ (shown in purple) is time-reversed and convolved with the upgoing wave field at $\mathbf{x}_B$ (shown in purple + green). In terms of traveltimes this means that the leg of downpropagation to $\mathbf{x}_A$ is subtracted from the total traveltime to reach $\mathbf{x}_B$ as an upgoing field. Consequently this results in the upgoing response of a downward radiating virtual source at $\mathbf{x}_A$, as we can see on the lefthand side of equation 3. In a similar fashion, we can derive that the acausal part of this operation results in a downgoing response of an upgoing virtual source. The interpretation of equation 4 is quite similar to equation 3 – see Figure 2b (note that equation 4 is the complex conjugate transpose of equation 3, meaning that all causal and acausal parts are interchanged). Equations 5 and 6 can be used to retrieve more complicated Green's functions, being upgoing / downgoing at both virtual source and receiver location. These Green's functions have seen both the medium below and above the receivers at least once – see Figures 2c and 2d. We will now demonstrate the use of these equations with a simple synthetic example.

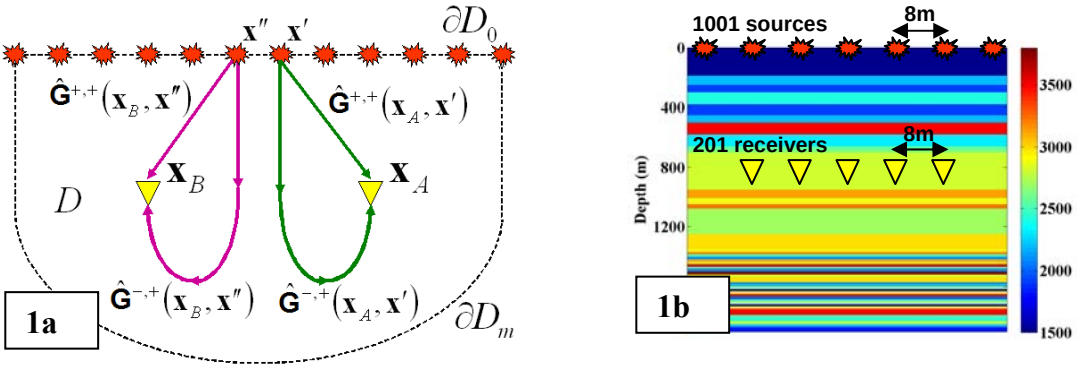

Figure 1a: *Configuration. Multi-component sources are located at level* ∂D_0*; multi-component receivers are located at* $\mathbf{x}_A$ *and* $\mathbf{x}_B$*. The decomposed Green's matrices between source* $\mathbf{x}'$ *and receiver* $\mathbf{x}_A$ *are given by* $\hat{\mathbf{G}}^{\pm,+}\left(\mathbf{x}_A,\mathbf{x}'\right)$*;* $\hat{\mathbf{G}}^{\pm,+}\left(\mathbf{x}_B,\mathbf{x}''\right)$ *represents the Green's matrix between source* $\mathbf{x}''$ *and receiver* $\mathbf{x}_B$*.* **1b:** *P-wave velocity and geometry: 1001 sources are located at the surface; 201 receivers are located at 800m depth.*

Example

In Figure 1b we show the P-wave velocity model and geometry for a simple synthetic 2D example. 201 multi-component receivers are placed at 800m depth, with 8m spacing. The earth's surface is covered with 1001 multi-component sources with 8m spacing. All free surface effects are eliminated by an absorbing boundary above the source array. The data are decomposed at the source and receiver side and cast into representation equation 1. First we construct the upgoing response of a downward radiating virtual source. In Figure 3a we show the PP-component of this operation (meaning the upgoing P-wavefield resulting from downward radiating P-wave virtual source, i.e. the upperleft element of $\hat{\mathbf{G}}^{-,+}$), compared to a directly modeled reference response. This result can be interpreted as a multi-dimensional extension of what was proposed by Mehta et al. (2007), who did not take wave conversion and flux-normalization into account. Note that we retrieve responses for the complete elastic system, as we demonstrate in Figure 3b, showing the upgoing S-wavefield converted from a downward radiating P-wave virtual source (i.e. the lower left element of $\hat{\mathbf{G}}^{-,+}$). With equation 4 we can generate upward radiating virtual sources to illuminate the medium above the receivers. As an example we show the downgoing S-wavefield of an upward radiating S-wave source (i.e. the lower right element of $\hat{\mathbf{G}}^{+,-}$).. Finally, we demonstrate the retrieval of more complicated Green's functions through equations 5 and 6. As an example, in Figure 4b we show that we can accurately retrieve even one of the weakest Green's functions with equation 6, being that of an upward radiating S-wave, converted to an upward P-wavefield (i.e. the upper right element of $\hat{\mathbf{G}}^{-,-}$).

Conclusion

We derived representations to redatum decomposed elatodynamic Green's functions to downhole receiver locations with great accuracy, as we demonstrated in an example. Required is that all free surface related effects have been removed from the data and that sufficient scattering occurs below the receiver array. The theory could be used for imaging both below and above the receiver array, as well as to retrieve more complicated multiple scattered waveforms.

Acknowledgements

This work is supported by the Dutch Technology Foundation STW, applied science division of NWO and the Technology Program of the Ministry of Economic Affairs (grant DCB.7913).

References

Bakulin, A., and Calvert, R., 2006, The Virtual Source method: theory and case study: Geophysics, **71**, SI139-SI150.
Mehta, K., Bakulin, A., Sheiman, J., Calvert, R., and Sneider, R., 2007, Improving the virtual source method by wave-field separation: Geophysics, **74**, V79-V86.
Schuster, G.T., 2009, Seismic interferoemtry: Cambridge University press; ISBN-13: 9780521871242.
Wapenaar, K., 2006, Green's function retrieval by cross-correlation in case of one-sided illumination: Geophysical Research Letters, **33**, L19304-1-L19304-6.
Wapenaar, K., Draganov, D., and Robertsson, J. (Editors) 2008, Seismic interferometry: History and present status: Society of Exploration Geophysicists Reprint Series **26**, ISBN 978-1-56080-150-4.

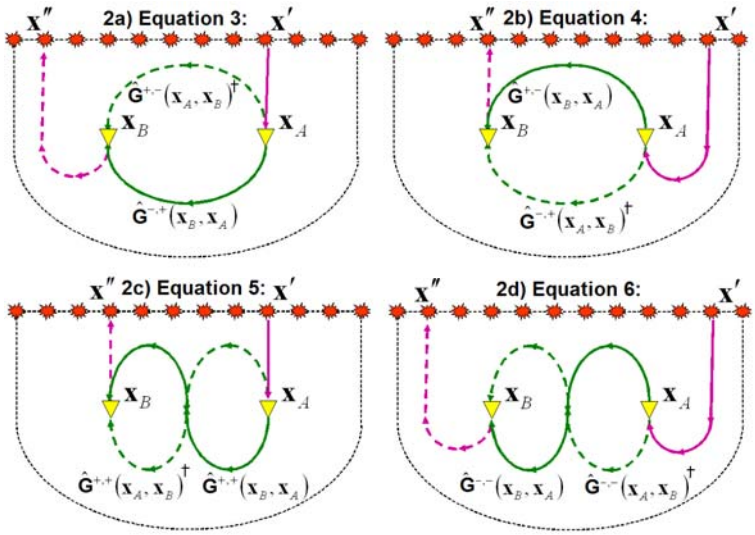

Figure 2: *Interpretations of the derived equations 3-6. Solid lines correspond to the reconstruction of causal Green's functions, dashed lines correspond to the reconstruction of acausal Green's functions. Green lines represent the retrieved responses, purple lines to the parts of the wave fields that are time-reversed. Locations* $\mathbf{x}'$ *and* $\mathbf{x}''$ *are illustrations of stationary points for the reconstructed causal and acausal Green's functions, respectively.*

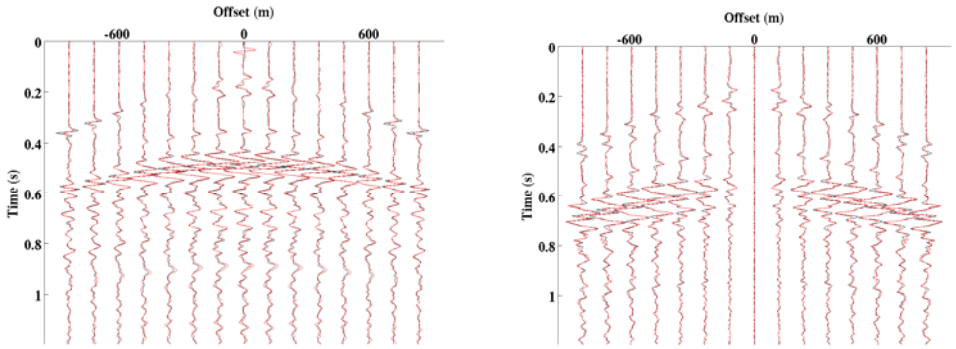

Figure 3a: *retrieved response (red) versus reference response (black) for an downgoing P-wave source and an upgoing P-wave receiver, using equation 3;* ***3b:*** *retrieved response (red) versus reference response (black) for an downgoing P-wave source and an upgoing S-wave receiver, using equation 3.*

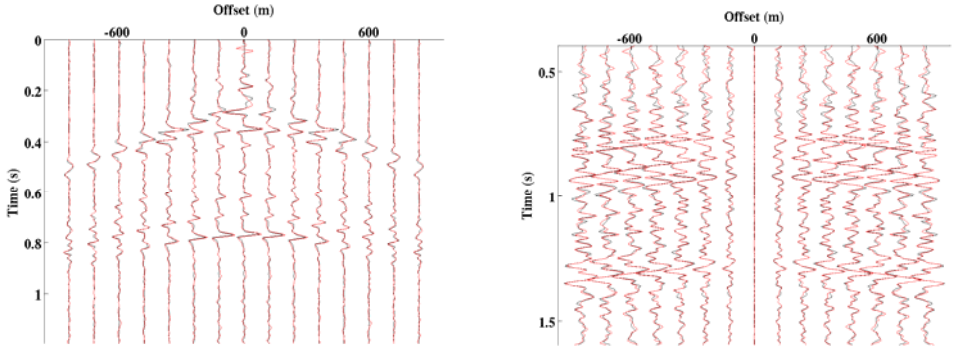

Figure 4a: *retrieved response (red) versus reference response (black) for an upgoing S-wave source and a downgoing S-wave receiver, using equation 4.* ***4b:*** *retrieved response (red) versus reference response (black) for an upgoing S-wave source and an upgoing P-wave receiver, using equation 6.*